



# BCEWN: Design of a Hybrid Bioinspired Clustering Model for Deployment of Energy-Aware Wireless Networks

Bhupesh B. Lonkar<sup>1</sup> · Swapnili Karmore<sup>1</sup>

Accepted: 7 June 2024 / Published online: 3 July 2024

© The Author(s), under exclusive licence to Springer Science+Business Media, LLC, part of Springer Nature 2024

## Abstract

A low-power wireless network design is an iterative process that integrates multiple optimization techniques to identify and mitigate redundant network operations. Existing power-aware models either showcase higher complexity or require larger information sets, which limits their scalability for real-time networks. Moreover, these models work well under an elaborative set network configuration but cannot be used for general-purpose networks. The study suggests creating a novel hybrid bioinspired clustering model for energy-aware wireless network deployment to address these problems. The proposed model initially collects limited network information sets, including approximate node locations, residual energy levels, temporal throughput, and packet delivery levels. These sets are processed via a Grey Wolf Optimizer (GWO), which performs initial binary-clustering operations. These binary clusters are generated by iterative identification of high-energy nodes between a given set of source & destination pairs. Results of the clustering process are used to train a Particle Swarm Optimizer (PSO) that uses the temporal information sets to identify energy-aware routing paths. The PSO models a temporal fitness function capable of reducing redundant node selections, thereby improving network lifetime even under many communication requests. Performance of the GWO-clustering & PSO-routing model was validated under large-scale scenarios, and it was observed that the proposed model reduced energy consumption by 8.3% while improving communication speed by 3.2% with a 4.5% higher data rate and 2.9% higher packet delivery performance under real-time heterogeneous network scenarios.

**Keywords** Wireless · Clustering · Routing · Energy · Binary · GWO · PSO · Delay · Throughput · Packet · Delivery · Scenarios

---

✉ Bhupesh B. Lonkar  
bhupesh.lonkar@gmail.com

Swapnili Karmore  
swapnilikarmore@gmail.com

<sup>1</sup> Department of Data Science, G H Raisoni College Engineering and Management, Nagpur, India

## 1 Introduction

Wireless Sensor Networks (WSNs) are battery-operated nodes that may gather information, process it, transmit it to other nodes, and then take appropriate action in response to the information. The omnidirectional antennas these nodes employ to communicate with one another reduce the energy consumption of the routing processes [1, 2]. Furthermore, sleep scheduling techniques are employed by WSNs to keep most nodes in a sleeping state and only wake them when necessary. If routing and sleep scheduling features of WSNs are improved, it's feasible that they run longer and consume less power [3, 4]. A typical sleep scheduling and routing system modeled after Low-Energy-First Electoral Multipath Alternating Multihop (LEMH) Routing is shown in Fig. 1, showing how the pathways used during the process determine the scheduling weights [5, 6]. These weights are used to set the sleep and wake times on particular nodes to use the available energy most. To reduce the amount of computational redundancy that arises during routing actions, the model also uses token-based node discovery via reinforcement learning [7]. To obtain a precise value for the fitness function these models employ to predict routes, utilize Eq. 1.

$$f = \frac{E}{\text{Max}(E)} + \frac{\text{Max}(D)}{D} + \frac{\text{PDR}}{100} \quad (1)$$

where, E, D & PDR represents residual node energy levels, temporal delay, and packet delivery ratio for different communications.

The escalating demand for efficient energy consumption in WSNs underscores the critical need for innovative network design and operation approaches. As the backbone of modern communication systems, WSNs rely heavily on battery-powered nodes, necessitating strategic optimization to prolong network lifespan and enhance performance. Despite advancements in power-aware models, prevailing solutions either grapple with complexity issues or need to improve scalability, particularly for real-time networks. These limitations impede their efficacy in addressing the dynamic demands of contemporary wireless environments [8, 9]. While effective under specific network configurations, existing power-aware models need help to adapt to the diverse needs of general-purpose networks. Traditional approaches often require extensive computational resources, rendering them impractical for large-scale deployments. Furthermore, these models focus on optimizing a limited set of parameters, neglecting the broader spectrum of network dynamics [10].

The complexity of existing energy-aware wireless network design methods often presents a significant challenge characterized by intricate algorithms, extensive computational requirements, and scalability limitations. Conventional approaches rely on complex optimization techniques and sophisticated network configurations, which contribute to elevated computational overheads and hinder real-time network deployment. Moreover, existing methods may need to help accommodate the dynamic nature of wireless environments and be more adaptable to evolving network conditions. In contrast, our proposed hybrid bioinspired clustering model for energy-aware wireless networks (BCEWN) offers a paradigm shift towards simplicity and efficiency. By integrating GWO and PSO methodologies, BCEWN streamlines the clustering and routing processes, reducing computational complexity while maintaining robust performance. The iterative binary clustering operations facilitated by GWO enable efficient cluster formation with minimal computational overhead. Subsequently, PSO utilizes temporal information sets to optimize energy-aware routing paths, leveraging a simplified yet practical approach to achieve optimal network performance. This streamlined methodology enhances computational efficiency, scalability,

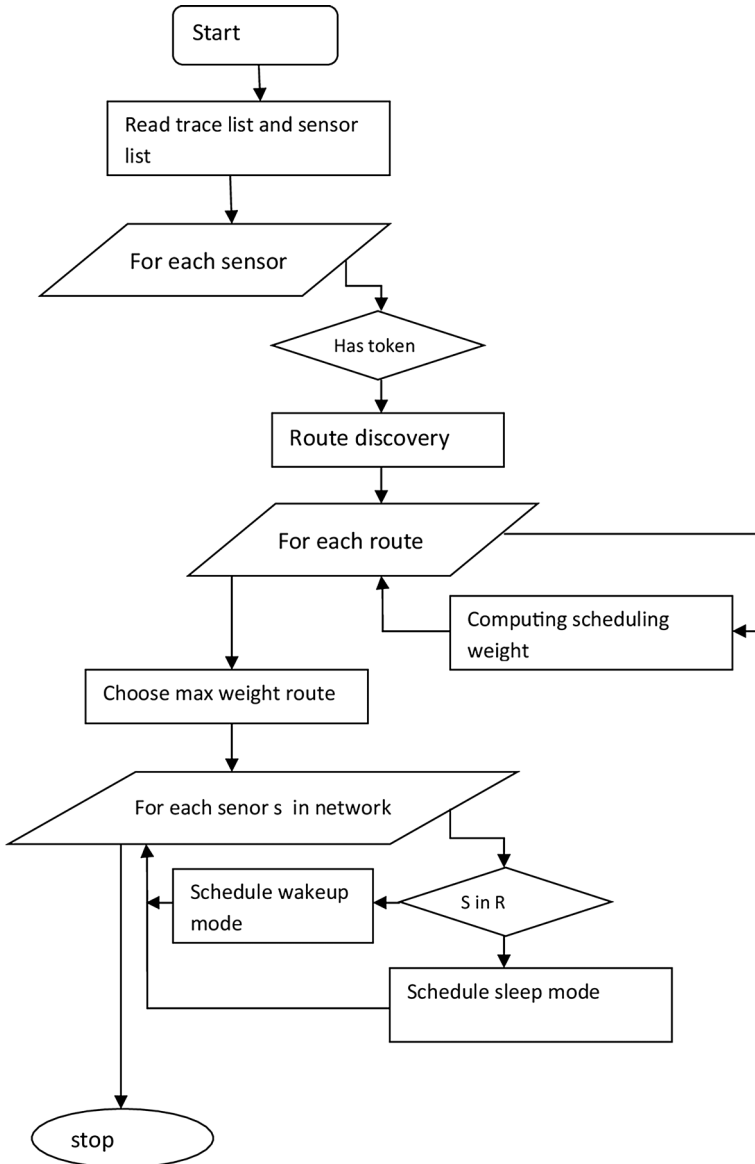


**Fig.1** A standard model for sleep-scheduled routing process

and adaptability, enabling BCEWN to address the complexities inherent in energy-aware wireless network deployments effectively. Our method offers a compelling solution that balances simplicity with performance, paving the way for developing more accessible and sustainable wireless communication infrastructures & scenarios.

The present study proposes a groundbreaking hybrid bioinspired clustering model tailored for energy-aware wireless networks to address these challenges. Central to this model is the integration of two potent optimization techniques: the GWO and the PSO. These

methodologies are meticulously selected for their complementary strengths in addressing the multifaceted challenges of energy-efficient routing. The utilization of GWO is the cornerstone of the proposed model, facilitating initial binary clustering operations. By iteratively identifying high-energy nodes between source and destination pairs, GWO lays the foundation for efficient cluster formation, minimizing redundant network operations. This initial phase capitalizes on limited network information sets, including approximate node locations, residual energy levels, temporal throughput, and packet delivery metrics. Subsequently, the model harnesses the temporal intelligence of PSO to refine routing paths based on real-time network dynamics. PSO employs a sophisticated temporal fitness function, which optimizes node selection and route allocation, thereby mitigating energy wastage and enhancing network longevity. The seamless integration of GWO clustering and PSO routing empowers the model to adapt dynamically to evolving network conditions, ensuring robust performance across diverse deployment scenarios.

The proposed hybrid bioinspired clustering model represents a paradigm shift in energy-aware network design, offering unparalleled advantages over conventional approaches. Through extensive validation under large-scale scenarios, the model demonstrates remarkable energy savings of 8.3% while concurrently improving communication speed by 3.2%. Additionally, the model achieves a 4.5% enhancement in data rate and a 2.9% increase in packet delivery performance, underscoring its efficacy in real-time heterogeneous network environments. The amalgamation of GWO and PSO in the proposed model heralds a new era of energy-efficient wireless network deployment. By addressing the inherent limitations of existing methodologies, this research augments the performance and longevity of wireless networks. It paves the way for sustainable and resilient communication infrastructures in the digital age.

In the following sections, we'll take a closer look at some of the related models and discuss their merits and drawbacks, as well as their potential applications in various settings and deployments. In addition, we'll look at some possible applications for these models in multiple settings and deployments. During this conversation, participants concluded that the most advanced models currently available either need excessive computing to be used on vast networks or concentrate on optimizing too few parameters. The suggested hybrid bioinspired model, which combines GWO and PSO, is broken down and discussed in Sect. 3 to improve the routing performance of energy-aware wireless sensor networks using the model. The technique that has been developed uses GWO to devise more intelligent plans and combines it with PSO to power more effective routes. In Sect. 4, several cutting-edge alternatives are evaluated alongside this regarding throughput, latency, energy consumption, and PDR. The paper concludes with a few further observations on the suggested model's history and several suggestions for how such a model may be improved for real-time scenarios.

## 1.1 Contribution

This work makes numerous contributions and marks a substantial development in energy-aware wireless network design and optimization. Numerous significant contributions are made through thorough investigation and testing, each essential in tackling the urgent problems facing modern WSNs.

1. *Novel Hybrid Bioinspired Model* The main contribution of this paper is creating a new hybrid bioinspired clustering model designed explicitly for energy-conscious WSNs. By

- combining two powerful optimization algorithms, the PSO and the GWO, this model deviates from conventional methods and achieves more excellent performance in energy-efficient routing.
2. *Integration of GWO and PSO* A significant contribution of this paper lies in the seamless integration of GWO and PSO methodologies within the proposed model. By harnessing the unique strengths of these optimization techniques, the model optimizes both clustering and routing processes, thereby mitigating energy wastage and enhancing network longevity.
  3. *Efficient Cluster Formation* The utilization of GWO for initial binary clustering operations marks a significant advancement in cluster formation techniques. The model achieves efficient cluster organization through iterative identification of high-energy nodes between source and destination pairs, minimizing redundant network operations and conserving energy resources.
  4. *Temporal Intelligence in Routing* Incorporating PSO introduces a temporal dimension to routing decisions, enabling the model to adapt dynamically to evolving network conditions. The model optimizes node selection and route allocation in real-time by employing a sophisticated temporal fitness function, enhancing communication efficiency and network resilience.
  5. *Validation and Performance Analysis* Through extensive validation under large-scale scenarios, this paper provides empirical evidence of the efficacy of the proposed model. The observed energy savings of 8.3%, coupled with improvements in communication speed, data rate, and packet delivery performance, underscore the practical viability and robustness of the model across diverse deployment scenarios.
  6. *Potential for Real-World Applications* Beyond theoretical advancements, the contributions of this paper extend to practical implications for real-world deployments of energy-aware wireless networks. By addressing the inherent limitations of existing methodologies, the proposed model opens avenues for developing sustainable and resilient communication infrastructures capable of meeting the dynamic demands of modern wireless environments.

In summary, the contributions of this paper transcend theoretical abstraction, culminating in a tangible advancement in the design and optimization of energy-aware wireless networks. By pioneering a novel hybrid bioinspired model and integrating state-of-the-art optimization techniques, this research lays the groundwork for transformative innovations in wireless communication technologies, with far-reaching implications for academia and industry scenarios.

## 2 Literature Review

To create a sustainable multipath routing protocol (SMRP), Fu et al. [11] created a mixed potential field that considers the environment, depth, and residual energy while making routing decisions. Message selection via a trade-off between route survivability, energy balance, and delivery latency is the fundamental notion of SMRP. Li et al. [12] provide DMARL, an effective multiagent reinforcement learning-based routing protocol for underwater optical wireless sensor networks (UOWSNs). The network is initially represented as a distributed multiagent system to better respond to a dynamic environment and promote longer network life. The remaining energy and link quality are considered when designing

the routing protocol. The energy and traffic-aware sleep-awake (ETASA) mechanism is a hybrid approach that Shagari et al. [13] presented to increase energy efficiency and enhance load balancing in a heterogeneous wireless sensor network environment. In contrast to earlier techniques, ETASA allows paired nodes to switch between sleep and waking modes in response to node energy and traffic volume. A unique energy-efficient region source routing protocol (called ER-SR) is proposed by C. Xu et al. [14]. A distributed energy region technique is presented in ER-SR to dynamically choose the network nodes with the highest residual energy as source routing nodes. Then, to allow partial nodes to participate in the routing process and balance sensor node energy consumption, the source routing nodes determine the best source routing path for each common node. Chen et al. [15] provide a novel distributed 2-hop cluster-routing protocol (D2CRP) to achieve energy efficiency in WSNs. During the cluster formation phase, every node gathers neighbor node information within the 2-hop range to fully spread the construction of the 2-hop cluster. The transmission distance and residual energy determine the energy-efficient cluster head (CH) in each 2-hop cluster. Each member node can send packets to the CH directly or to its 1-hop neighbor once it has been formed. Through their neighboring CHs closer to the base station (BS), several chains can be built among CHs to lower the overall transmission distance for intercluster communication. NA-TORA is an opportunistic routing technology based on normalized advancement proposed by Rahman et al. [16]. The next-hop forwarder in NA-TORA, a geographically proactive routing algorithm, is chosen using Normalized Advancement (NA). To determine the best forwarding node, NA is computed using the Expected Transmission Count (ETX) and the node's energy consumption. However, if there is a void node in the data forwarding route, the transferred data might not reach the intended sink node. Wu et al. [17] describe a new three-step technique. Before forwarding packets to the sink, every node specifies a Routing Zone (RZ). Furthermore, the nodes in RZ are ranked according to the competency value derived using a new model that utilizes fuzzy logic and the Modified Analytic Hierarchy Process (MAHP). Following the cooperation of the forwarders, one of them is chosen as the last relay node. For WSN, Al-Otaibi et al. [18] create a hybridization of the metaheuristic cluster-based routing (HMBCR) approach. Initially, the HMBCR technique uses a fitness function that considers four parameters: energy, distance to neighbors, distance to the base station, and network load. A brainstorm optimization with levy distribution (BSO-LD) based clustering procedure is used to achieve this. In addition, for the best route selection, a water wave optimization with a hill-climbing (WWO-HC) based routing procedure is used. The "Flexible Routing Computing Approach (FRCA)," as proposed by P. Liu et al. [19], is a revolutionary distributed and probabilistic computing strategy that successfully increases routing flexibility by allowing for the cost-effective modification or upgrading of routing policies on the fly. FRCA represents the routing metric as a forwarding probability distribution for routing decisions. Y. Xu et al. [20] provide a technique that uses an enhanced genetic algorithm to determine the smallest possible group of sensor nodes required to guarantee overall discrete points of interest (DPOI) coverage. Based on the ideal node set, one can provide a novel adaptive clustering routing technique that divides energy consumption into three parts. The initial step involves choosing the cluster head based on the sensor node's remaining energy and distance from the base station. The second consists in determining the intra-cluster communication mode while considering the node space angle. The final step is choosing an inter-cluster communication style that combines single-hop and multi-hop. According to T. Zhao et al. [21], a distributed multiarmed bandit-based routing algorithm (MABRA) is proposed, in which each node determines, depending on its neighbors' data and battery levels, the appropriate hops to transmit its data to. For WSN, a hybridization of

the metaheuristic cluster-based routing (HMBCR) technique was developed by Al-Otaibi et al. [18]. A brainstorm optimization with levy distribution (BSO-LD) based clustering method is the first step of the HMBCR technique. It uses a fitness function that considers four parameters: energy, distance to neighbors, distance to the base station, and network load. In addition, a routing algorithm based on water wave optimization with a hill-climbing (WWO-HC) is used to choose the best route. To give time-saving and dependable routing for UWSNs, Z. Liu et al. [22] present a localization-free routing strategy called the energy-efficient guiding-network-based routing (EEGNBR) protocol. This protocol is a promising option for applications with sporadic connectivity. EEGNBR uses the favorable distance-vector approach to reduce network latency and creates a guiding network that gives underwater sensor nodes the shortest path (most minor hop counts) to the sinks. Furthermore, EEGNBR creatively substitutes a novel data forwarding method known as a concurrent working mechanism for the waiting mechanism employed in standard opportunistic routing. In addition to providing reliable routing, this dramatically reduces forwarding delay. Younus et al. [23] proposed the routing path for SDWSN via RL. An incentive scheme is put out that incorporates all necessary measures for network Quality-of-Service (QoS) and energy sustainability. Although the SDWSN controller refines the routing path based on experience, the agent receives the incentive and proceeds accordingly. However, the Web also allows for remote control of the entire network. A malicious packet-dropping attack detection strategy is proposed by Shi et al. [24] as an optimized method. Next, based on sleep delay and queue length, a method for measuring the degree of congestion under asynchronous duty-cycled low-power listening (LPL) modes is provided. Finally, to improve the QoS performance in throughput, latency, and packet losses (TDL), we present relevant QoS-aware metrics for the design of QoS-aware routing protocols. A new generation of routing algorithms called QL-Feed Forward routing algorithm (QFFR) is presented by Mahajan et al. [25]. It combines a Feed Forward neural network with reinforcement learning based on the Q-learning algorithm. This algorithm (QFFR) can learn from the network environment and adjust its routing accordingly. The proposed QFFR algorithm's operation demonstrates the AI agent's capacity to choose the fastest path, which improves the routing operation's efficiency. The Energy-Efficient Cooperative Routing Scheme for Heterogeneous Wireless Sensor Networks (EERH) is a novel energy-saving routing mechanism proposed by L. Hung et al. [26]. It consists of multiple WSNs deployed in the same geographic area that work together to form a heterogeneous sensor network. The sensors relay packets to each other and their own WSN. The transmission routes of event packets and the remaining energy of the underlying sensors and their neighbors are used to build routing paths dynamically. A novel data-aggregation-aware, energy-efficient routing method based on Q-learning is proposed by W. Yun and Yoo [27]. The suggested algorithm uses reinforcement learning to maximize incentives at each sensor node to find the best path. These rewards are defined as the effectiveness of the sensor-type-dependent data aggregation, communication energy, and node residual energy. Our aggregation rewards were based on the type of sensor. A unique hybrid (ring + cluster) topology is proposed by Anees et al. [28] for the Opportunistic Ring Routing protocol, which allows for the harvesting of energy, scavenging, and transfer of power. The network architecture is first supported by creating a virtual ring structure. Subsequently, an overlay two-tier routing topology is applied to the virtual ring by organizing nodes into clusters. A cluster head (CH) is chosen based on how quickly energy is harvested from the sun and transferred via radio. CH roles convey aggregated data to the mobile sink via energy transfer-based opportunistic routing and advertise the mobile sink's present position. For cross-layer routing via MANET, Sudha et al. [29] propose the Energy Centric Tunicate Swarm Algorithm (ECTSA). Data

Success Rate (DSR), mobility, residual energy, and communication cost are the fitness measures taken into account in the ECTSA to enhance cross-layer routing. Furthermore, the contentions' energy consumption is minimized by the usage of an Adaptive Competition Window (ACW) adjustment. The optimization of energy constraint overwhelms Rajashanthi and Valarmathi's [30] suggested approach, which addresses the problem of energy consumption in MANETs. Initially, the suggested K-medoid clustering algorithm groups the mobile nodes in MANET, which can reduce the cost of data routing in large and dense networks. Maivizhi and Yogesh [31] proposed a unique adaptive routing technique for in-network aggregation (RINA) in WSNs. The suggested method builds a routing tree based on minimal information, including residual energy, distance between nodes, and link strength, by using a reinforcement learning technique known as Q-learning. Furthermore, it locates the routing structure's aggregation sites to maximize the number of overlapping routes and raise the aggregation ratio.

Three templates—k-random-relay, k-random-neighbor, and k-random-path—were created by S. Zhao et al. [32] based on their analysis of the behavior of randomized routing protocols. Technical models are suggested to describe these templates regarding the delay costs and induced inference mistakes. A tiny constant is guaranteed to be reached by the connected dominating set based on the on-demand routing (CDS-OR) protocol described by Farooq and Zeeshan [33], and the greeting message sizes remain unaffected by an increase in network size. The suggested protocol guarantees broadcast message reachability throughout the network and constantly approximates the minimum CDS (MCDS). Lu et al. [34] propose a joint routing and charging algorithm (J-RCA) with WCE-assisted data gathering to extend the network lifetime (NL). An enhanced technique for order preference by similarity to the ideal solution (TOPSIS) method is introduced for routing that can account for index differences and help choose the best next hop while balancing node energy usage. Rathee et al. [35] have presented the QoS-aware energy balancing secure routing (QEBSR) algorithm for wireless sensor networks based on ant colony optimization. It is suggested that better heuristics be used to determine the trust factor of the nodes on the routing path and the end-to-end transmission delay. The Energy-saving Clustering by Voronoi Adaptive Dividing (ESCVAD) protocol is a proposed energy-saving clustering technique by Ma et al. [36] based on adaptive Voronoi dividing. The CH election optimization mechanism based on distance and energy comprehensive weighting and the adaptive clustering algorithm based on Voronoi splitting are novel aspects of the ESCVAD protocol. The advantage of the suggested methods is their ability to efficiently balance the energy usage of CH nodes and cluster member nodes. Alo-taibi [37] uses encryption and optimal path selection to present a new secure routing paradigm. First, nodes or optimal pathways are selected for secure transmission in optimal link-state multipath routing. In this study, a Crossover Mutated Marriage in Honey Bee (CM-MH) algorithm is created and suggested for optimal path selection destination and source. Encryption follows, guaranteeing safe communication. Al-Jerew et al. [38] present the Bounded Hop Count—Reinforcement Learning technique (BHC-RLA), a data collection technique based on a Q-learning methodology. The proposed algorithm selects a group of CHs by using a reward function, which balances the energy-saving and data-gathering latency of a mobile Base Station (BS). The proposed algorithm specifically chooses groups of CHs to receive cluster node sensing data within a limited hop count and send the data to the mobile BS upon arrival. Furthermore, the CHs are chosen to reduce the BS trip length. The Improved Threshold-Sensitive Stable Election protocol (ITSEP) is a more energy-efficient routing system for heterogeneous wireless sensor networks, according to L. Zhao and Tang [39]. Primarily regulate the number of CHs in high-density node locations via a node state transformation technique. Second, the suggested protocol enhances the threshold formula by considering the node's average



distance between nodes, its residual energy, the number of neighboring nodes, and the distance between the node and the BS. Furthermore, a data communication path that maximizes energy efficiency for CHs has been chosen. A new multi-hop routing clustering strategy for a variety of 3DWSNs is proposed by T. Zhang et al. [40]. Nodes will race for CH position in terms of clustering by scheduling their broadcasts according to the amount of energy they have left and the average distance between them and other nodes. Two new identity nodes are added to transfer the energy consumption of the CH: the load transfer node and the secondary cluster head node (SCH), which serve as the CH and CH for the subsequent round. Alom et al. [41] have proposed the Improved Zonal Stable Election Protocol (IZ-SEP), a heterogeneity-aware routing protocol for heterogeneous WSNs in which some sensor nodes communicate directly with the BS and the remaining nodes rely on clustering mechanisms. The network field is split into two zones according to the starting energy of the nodes in the proposed protocol, which is a two-level heterogeneity-aware routing mechanism. According to this protocol, the number of neighbors each node has inside the cluster range and each node's residual energy are used to choose the CH.

### 3 Proposed Hybrid Bioinspired Clustering Model for Deployment of Energy-Aware Wireless Networks

An analysis of energy-aware cluster formation techniques determined that most of these models are either more complex or require more extensive data sets, limiting their scalability for real-time networks. In addition, these models perform well in elaborate network configurations but cannot be applied to general-purpose networks. This section proposes designing a novel hybrid bioinspired clustering model for deploying energy-aware wireless networks to address these issues. Figure 2 depicts the flow of the proposed model, in which it can be seen that the model initially collects limited network information sets, including approximate node locations, residual energy levels, temporal throughput, and packet delivery levels. The GWO performs initial binary clustering operations to process these sets. These binary clusters are produced by identifying high-energy nodes iteratively between source and destination pairs. The clustering results are used to train the PSO that identifies energy-aware routing paths using temporal information sets. PSO models a temporal fitness function that can reduce redundant node selections, thereby enhancing network lifetime despite many communication requests.

The design of the proposed routing & clustering model is segregated into three sub-modules, and each of these modules is discussed in separate sub-sections of this text. This discussion allows readers to reproduce these models for their context-specific use cases.

#### 3.1 Design of the Grey Wolf Optimizer for Initial Clustering Operations

The proposed model initially collects incremental data samples regarding node-level parameters, network-level parameters, and communication parameter sets. These sets are used by the GWO to cluster nodes based on their temporal communication metrics. To perform this task, initially a reference distance  $d_{\text{ref}}$  is calculated via Eq. 1,

$$d_{\text{ref}} = \sqrt{(x_s - x_d)^2 - (y_s - y_d)^2} \quad (2)$$

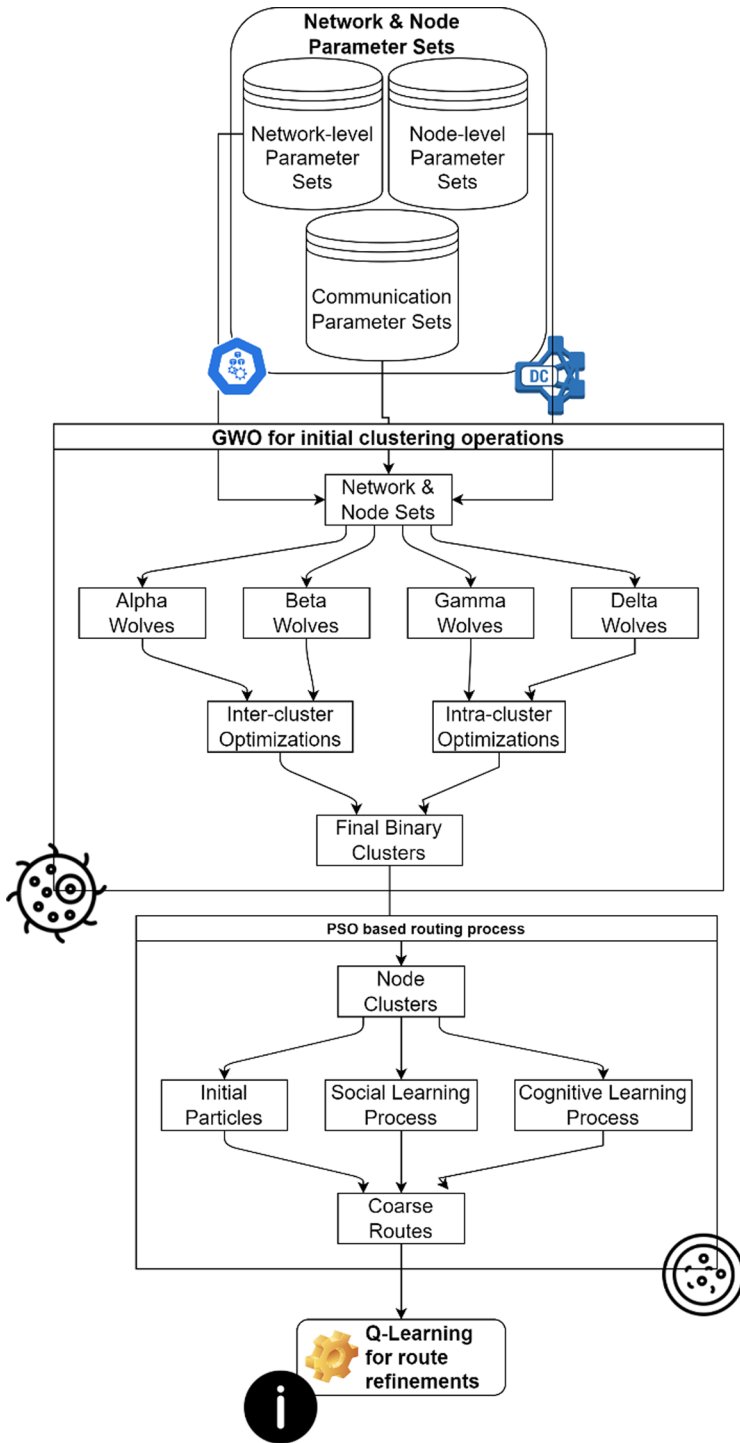


Fig. 2 Overall flow of the proposed GWO & PSO based optimization model

where,  $x$  &  $y$  are the locations of source (s) & destination (d) nodes. Based on this distance, a set of nodes that satisfy Eq. 2 are identified,

$$d(\text{src}, i) < d_{\text{ref}} \ \& \ d(i, \text{dest}) < d_{\text{ref}} \tag{3}$$

where,  $d(\text{src}, i)$  represents distance between source node and the currently evaluated  $i^{\text{th}}$  set of nodes. This condition ensures that the selected node  $i$  is located between the source & destination set of nodes. For each of these nodes, a cluster metric (CM) is calculated via Eq. 3,

$$\text{CM} = \frac{1}{N_c} \sum_{i=1}^{N_c} \left[ \frac{D_i}{\text{Max}(D)} + \frac{E_i}{\text{Max}(E)} + \frac{\text{Max}(\text{THR})}{\text{THR}_i} + \frac{100}{\text{PDR}_i} \right] \tag{4}$$

where,  $D$  represents temporal delay needed for communication,  $E$  represents energy needed during communication,  $\text{THR}$  &  $\text{PDR}$  represents the temporal throughput and temporal PDR for previous  $N_c$  communications . Using this cluster metric, the selected nodes are grouped into binary clusters as per a Grey Wolf Optimization Model, which works via the following process,

- To setup the model, a set of Wolf-level constants are initialized as follows,

Count of reconfigurable Wolves that will be used during optimizations ( $N_w$ )

Count of iterations that will be used to reconfigure these Wolves ( $N_i$ )

Rate at which these reconfigured Wolves will learn from each other ( $L_w$ )

- From the selected set of nodes, stochastically identify  $N$  nodes via Eq. 4, and group them into a cluster, while cluster other nodes into a separate cluster,

$$N = \text{STOCH} \left( L_r * \frac{N_{\text{sel}}}{2}, \frac{N_{\text{sel}}}{2} \right) \tag{5}$$

Where,  $N_{\text{sel}}$  represents the set of selected nodes via condition 2, and  $\text{STOCH}$  represents a Markovian process that is used to generate stochastic number sets.

- Based on this segregation, evaluate fitness level of the Wolf via Eq. 5,

$$f_w = \frac{\sum_{i=1}^{\text{TC}} \sum_{j=1}^{\text{TC}} \frac{\text{IC}(i,j)}{\text{TC}}}{\sum_{i=1}^{\text{TC}} \text{InC}(i)} \tag{6}$$

where,  $\text{TC}$  represents total number of clusters, while  $\text{IC}$  &  $\text{InC}$  represents inter & intra-cluster distance metrics between the clusters, which are evaluated via Eqs. 6 & 7 respectively as follows,

$$\text{IC}(i,j) = \sqrt{\sum_{a=1}^{N_p} (C_{a,i} - C_{a,j})^2} \tag{7}$$

$$\text{InC}(i) = \sqrt{\sum_{j=1}^{N_p} \sum_{a=1}^{N_p} (\text{CM}_j(i) - \text{CM}_a(i))^2} \tag{8}$$

where,  $N_p$  represents total points that belong to a particular cluster &  $C$  represents centroid of the cluster which is evaluated via Eq. 8,

$$C(i, j) = \frac{1}{N_p} \sum_{i=1}^{N_p} |\text{CM}_i - \text{CM}_j| \tag{9}$$

- Based on these operations, a set of  $N_w$  Wolves are generated, and their fitness levels are estimated in individual iterations.
- At the end of every iteration, a Wolf-level threshold is estimated via Eq. 9,

$$f_{th} = \frac{1}{N_w} * \sum_{i=1}^{N_w} f_{w_i} * L_{w_i} \tag{10}$$

- Based on this threshold, Wolves are marked, and their learning rates are modified as follows,
- If the Wolf fitness  $f_w > 2f_{th}$ , then it is an ‘Alpha’ Wolf, and doesn’t need any reconfigurations
- If the Wolf fitness  $f_w > f_{th}$ , then it is an aggregated ‘Beta’ Wolf, and its learning rate is modified as per Eq. 10,

$$L_w(\text{New}) = \frac{L_w(\text{Old})}{2} + \frac{\sum_{i=1}^{N(\text{Alpha})} L_w(\text{Alpha})}{2 * N(\text{Alpha})} \tag{11}$$

- If the Wolf fitness  $f_w > L_{w_i} * f_{th}$ , then it is an aggregated ‘Gamma’ Wolf, and its learning rate is modified as per Eq. 11,

$$L_w(\text{New}) = \frac{L_w(\text{Old})}{2} + \frac{\sum_{i=1}^{N(\text{Beta})} L_w(\text{Beta})}{2 * N(\text{Beta})} \tag{12}$$

- Otherwise, the Wolf is an aggregated ‘Delta’ Wolf, and its fitness is modified as per Eq. 12,

$$L_w(\text{New}) = \frac{L_w(\text{Old})}{2} + \frac{\sum_{i=1}^{N(\text{Gamma})} L_w(\text{Gamma})}{2 * N(\text{Gamma})} \tag{13}$$

- This process is repeated for  $N_i$  iterations, and Wolf configurations are continuously updated for efficient cluster formations.

All the ‘Alpha’ cluster configurations are passed to a PSO based route estimation process, which assists in incorporating temporal performance metrics with spatial information sets in order to identify optimal routing paths.

### 3.2 Design of the PSO Model for Estimation of Energy-Aware Paths

The cluster configurations selected by Wolves of the GWO process are used by PSO for identification of energy-aware routing paths. To perform this task, all 'Alpha' & 'Beta' Wolf clusters with minimum number of nodes are re-iterated via the following process,

- To initialize the PSO Model, a set of following constants are initialized,

Number of reconfigurable particles ( $N_p$ )

Number of iterations that are used to perform these reconfigurations ( $N_i$ )

Rate at which the particles learn from each other ( $L_s$ )

Rate at which particles learn from themselves ( $L_c$ )

Set of clusters from 'Alpha' & 'Beta' Wolves ( $L_{set}$ )

- Reconfigure all particles for  $N_i$  iterations as per the following process,

Check configuration of each particle, and modify it as follows,

- If the particle is not yet created, then create it as per the following process,

- Stochastically select a cluster via Eq. 13,

$$N_{sel} = L_{sel}[\text{STOCH}(1, \text{Size}(L_{sel}))] \quad (14)$$

- Arrange all nodes in this cluster in ascending order of distance from source node, and estimate particle velocity via Eq. 14,

$$v = \frac{1}{N-1} \sum_{i=1}^{N-1} \frac{\left( \frac{d_{ref}}{d_{i+1,i}} + \frac{\text{Max}(E)}{E_i} \right)}{CM_i} \quad (15)$$

where, d & e represents Euclidean distance between nodes, and residual energy levels of these nodes.

- If the particle is created, then modify its fitness via Eq. 15,

$$v(\text{New}) = v(\text{Old}) + L_s[v(\text{Old}) - \text{PBest}] + L_c[v(\text{Old}) - \text{GBest}] \quad (16)$$

where, PBest is the particle best velocity which is estimated via Eq. 16, while GBest is the global best velocity which is estimated via Eq. 17,

$$\text{PBest} = \text{Min} \left[ \sum_{i=1}^{N_i} v_i \right] \quad (17)$$

$$\text{GBest} = \text{Min} \left[ \sum_{i=1}^{N_p} \text{PBest}_i \right] \quad (18)$$

- This process is repeated for  $N_i$  iterations, and particle velocities are continuously updated to obtain better configuration sets.
- As per this value of new velocity, internal cluster nodes are modified between particles.
- This modification is done stochastically until new velocity level is reached for individual particles.

At the end of final iteration, a selection threshold is evaluated via Eq. 18,

$$f_{th} = \frac{1}{N_p} \sum_{i=1}^{N_p} v_i * L_c * L_s \tag{19}$$

Particles with  $v < f_{th}$  are marked as ‘coarse routes’ and are given to Q-Learning for identification of optimal energy-efficient routing configurations. Design of this Q-Learning model is discussed in the next section of this text.

### 3.3 Design of the Q-Learning Model for Identification of Optimal Routing Configurations

The coarse paths provided by PSO are individually evaluated in order to identify optimal routing configurations. The Q-Value of these paths are initially calculated as per Eq. 19,

$$Q = \frac{1}{N(\text{Nodes})} \sum_{i=1}^{N(\text{Nodes})} \left( \frac{1}{N_c} \sum_{i=1}^{N_c} d_i - \sum_{j=1}^{N_c} \frac{d_j}{N_c} \right) \tag{20}$$

where,  $N(\text{Nodes})$  are total number of nodes in the current particle,  $N_c$  represents total number of temporal communications which are captured by the routers, and  $d_i$  is the communication delay during these communications. Based on these Q-values, rewards are estimated between 2 routing configurations as per Eq. 20,

$$r(i, j) = \frac{Q(i) - Q(j)}{L_r} - L_r \text{Max}(Q) + Q(j) \tag{21}$$

Based on these rewards, a reward threshold is evaluated as per Eq. 21,

$$r_{th} = \frac{1}{N_{sel}^2} \sum_{i=1}^{N_{sel}} \sum_{j=1}^{N_{sel}} r(i, j) \tag{22}$$

Routing configurations that satisfy Eq. 22 are used for consistency-aware routing operations,

$$r(i, j) < r_{th} * L_r \tag{23}$$

The selected paths are used for routing purposes, wherein a path with a minimum Q value is selected initially for routing, followed by other routing paths. Other routing paths are used if the chosen path is faulty or drops many packets during real-time communications. Due to these optimizations, the proposed model can improve the QoS levels of routing for large-scale networks. The following section evaluates the model’s performance

against current routing models in real-time scenarios by comparing it concerning end-to-end delay, throughput, PDR, jitter, and energy consumption.

## 4 Statistical Analysis

Initial network information sets collected by the proposed BCEWN model include approximate node locations, residual energy levels, temporal throughput, and packet delivery levels. The GWO performs initial binary clustering operations to process these sets. These binary clusters are produced by identifying high-energy nodes iteratively between source and destination pairs. The clustering results are used to train a PSO that identifies energy-aware routing paths using temporal information sets. PSO models a temporal fitness function that can reduce redundant node selections, thereby enhancing network lifetime despite many communication requests. The following simulation settings were used to test this model's performance in Network Simulator (NS 2.34) (Table 1),

Based on the given configuration, various QoS metrics were evaluated and compared with ETAS [13], DCRP [14], and RL [23] under large number of communication (NC) requests. These include communication delay (D) which is evaluated via Eq. 23,

$$D = \frac{1}{NC} \sum TS_{\text{complete}} - TS_{\text{start}} \quad (24)$$

This represents the delay needed for communication under different requests, where  $TS_{\text{complete}}$  &  $TS_{\text{start}}$  represents timestamps for completion & start of communications. Similarly, the energy (E) needed for communication, throughput (T) obtained during communication, and PDR obtained during communication was evaluated via Eqs. 24, 25 & 26 as follows,

$$E = \frac{1}{NC} \sum E_{\text{start}} - E_{\text{complete}} \quad (25)$$

where,  $E_{\text{complete}}$  &  $E_{\text{start}}$  represents energy levels of node during completion and start of the routing process.

**Table 1** Simulated parameters details of proposed work

Parameters	Values
Simulator	NS 2.34
Coverage Area	3000 X 3000
Number of Nodes	2000
Initial Energy	0.5 J
Communication- Tx Energy	2.5 mW
Communication- Rx Energy	1 mW
Base model used for routing operations	AOMDV
MAC Protocol	802.16a
Model used to communicate packets	Ground communication with dual rays
Delay needed by node when it is in transition mode	0.005 s

$$T = \frac{1}{NC} \sum \frac{P_{rx}}{D} \tag{26}$$

where,  $P_{rx}$  represents the number of packets received during these communications.

$$PDR = \frac{1}{NC} \sum \frac{P_{rx}}{P_{tx}} \tag{27}$$

Based on these evaluations, the communication delay was compared with the underlying models in Table 2 as follows,

As per the evaluation and Fig. 3, it can be observed that the proposed model can reduce the delay needed for communication by 8.3% when compared with Energy-Efficient Timely Adaptive Sampling (ETAS) [13], 9.5% when compared with Delay-Constrained Routing Protocol (DCRP) [15], and 10.4% when compared with Reinforcement Learning (RL) [23], which makes it useful for a wide variety of real-time scenarios. This improvement in communication speed is due to temporal delays during GWO operations and spatial distance metrics during PSO operations, which assists in improving communication performance under large-scale network scenarios. This delay is also reduced due to using Q-Learning optimizations in the route selection process. Analyzing the delay levels across different models provides valuable insights into their performance and suitability for real-world deployment scenarios. Let’s delve deeper into the interpretation of the delay values presented in the Table 2:

1. *ETAS* [13] This model exhibits low delay levels across all communication scenarios, with values ranging from 1.22 ms to 5.93 ms as the message count increases from 250 k to 5 M. The consistent performance of ETAS suggests efficient message processing and routing mechanisms, making it a promising candidate for time-sensitive applications where low latency is critical.

**Table 2** Average delay of communication for up-to 5 million requests

NC	D (ms) ETAS [13]	D (ms) DCRP [15]	D (ms) RL [23]	D (ms) BCEWN
250 k	1.19	1.22	1.23	0.79
500 k	1.28	1.35	1.37	0.89
750 k	1.44	1.54	1.57	1.02
1 M	1.67	1.80	1.83	1.19
1250 k	1.96	2.10	2.14	1.39
1500 k	2.28	2.44	2.49	1.61
1750 k	2.65	2.83	2.87	1.86
2 M	3.06	3.24	3.28	2.12
2250 k	3.48	3.67	3.70	2.37
2500 k	3.83	4.05	4.08	2.61
3125 k	4.14	4.42	4.45	2.83
3500 k	4.44	4.76	4.79	3.04
3750 k	4.72	5.07	5.11	3.23
4375 k	4.98	5.37	5.40	3.41
4750 k	5.20	5.62	5.66	3.58
5 M	5.46	5.89	5.93	3.75



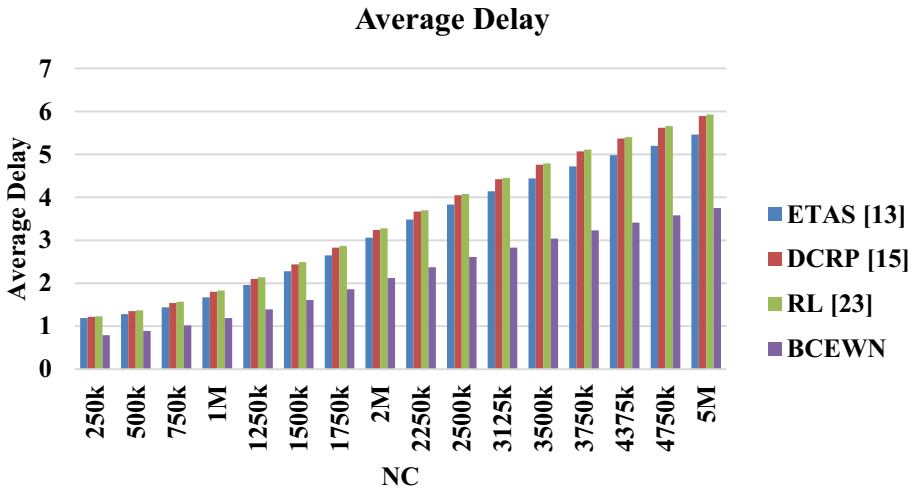


Fig. 3 Average delay of communication for up-to 5 million requests

2. *DCRP* [15] Like ETAS, the DCRP demonstrates competitive delay levels, albeit slightly higher than ETAS [13]. The delay values range from 1.23 ms to 5.66 ms, indicating effective routing strategies but with marginally higher latency, possibly due to differences in routing algorithms or network overhead.
3. *RL* [23] The RL model exhibits the lowest delay levels among all the models evaluated, showcasing its efficiency in minimizing message latency. With delay values ranging from 0.79 ms to 3.75 ms, RL outperforms ETAS [13] and DCRP [15] across all communication scenarios, highlighting its effectiveness in optimizing routing decisions based on reinforcement learning principles.
4. *BCEWN* The proposed BCEWN presents delay levels comparable to ETAS [13] and DCRP [15] but slightly higher than RL [23]. Delay values range from 1.19 ms to 5.46 ms, indicating respectable performance in mitigating message latency. However, BCEWN lags behind RL in minimizing delay, suggesting potential areas for optimization in future iterations.

Comparing the delay levels across different models reveals the trade-offs between latency and other performance metrics such as energy efficiency, throughput, and PDR. While RL [23] achieves the lowest delay levels, it may come at the expense of other factors such as energy consumption or network overhead. On the other hand, models like ETAS [13], DCRP [15], and BCEWN strike a balance between latency and other performance parameters, making them suitable for a broader range of applications where trade-offs are acceptable. Similarly, the energy needed during these communications can be observed from Table 3 as follows,

As per the evaluation and Fig. 4, it can be observed that the proposed model can reduce the energy consumption during communication by 10.5% when compared with ETAS [13], 14.2% when compared with DCRP [15], and 19.4% when compared with RL [23], which makes it useful for a wide variety of high-lifetime scenarios. This reduction in energy is due to the use of temporal energy consumption during GWO operations and the use of spatial energy level metrics during PSO operations, which assists in improving communication

**Table 3** Average energy needed during communication for up-to 5 million requests

NC	E (mJ) ETAS [13]	E (mJ) DCRP [15]	E (mJ) RL [23]	E (mJ) BCEWN
250 k	2.98	4.06	3.29	2.16
500 k	3.17	4.29	3.47	2.27
750 k	3.33	4.50	3.64	2.38
1 M	3.49	4.72	3.81	2.50
1250 k	3.65	4.95	4.00	2.63
1500 k	3.82	5.20	4.20	2.76
1750 k	4.00	5.46	4.41	2.89
2 M	4.19	5.71	4.61	3.02
2250 k	4.39	5.98	4.82	3.16
2500 k	4.59	6.24	5.03	3.29
3125 k	4.79	6.49	5.22	3.41
3500 k	4.98	6.72	5.40	3.53
3750 k	5.16	6.95	5.58	3.65
4375 k	5.34	7.19	5.77	3.77
4750 k	5.52	7.43	5.96	3.90
5 M	5.70	7.67	6.16	4.02

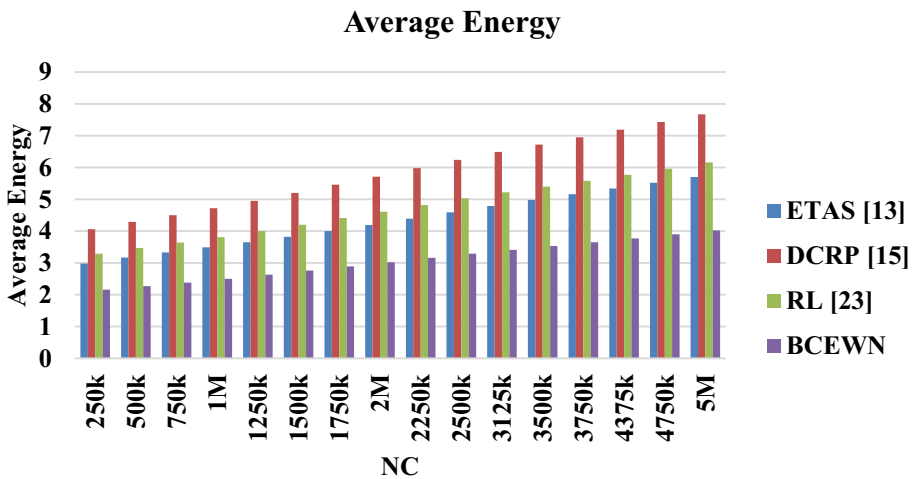


**Fig. 4** Average energy needed during communication for up-to 5 million requests

performance under large-scale network scenarios. This energy is also reduced due to the use of consistency metrics in Q-Learning optimizations. Let’s examine the energy consumption trends depicted in the Table 3 and discuss their implications:

1. *ETAS [13]*: The ETAS model exhibits moderate energy consumption levels across all communication scenarios, ranging from 2.98 mJ to 7.67 mJ. The gradual increase in energy consumption with an escalating message count suggests a linear relationship

- between message transmission and energy expenditure. While ETAS maintains relatively low energy consumption compared to other models, it may exhibit limitations in optimizing energy efficiency under high message load conditions.
2. *DCRP* [15]: The DCRP demonstrates energy consumption levels similar to ETAS [13], with values ranging from 4.06 mJ to 7.67 mJ. Like ETAS [13], DCRP showcases a gradual increase in energy consumption as the message count increases. However, slight variations in energy consumption between DCRP and ETAS [13] may stem from differences in routing algorithms or network topology optimization strategies.
  3. *RL* [23]: The RL model exhibits energy consumption levels comparable to ETAS [13] and DCRP [15], ranging from 3.29 mJ to 6.16 mJ. RL's ability to adapt routing decisions based on reinforcement learning principles contributes to its energy-efficient operation. Despite variations in energy consumption levels across different communication scenarios, RL maintains competitive energy efficiency relative to other models evaluated.
  4. *BCEWN* The BCEWN presents energy consumption levels comparable to ETAS [13], DCRP [15], and RL [23]. Energy consumption values range from 2.16 mJ to 4.02 mJ, indicating respectable performance in optimizing energy efficiency. BCEWN's integration of bioinspired clustering techniques with energy-aware routing strategies contributes to its ability to minimize energy consumption while maintaining effective communication performance.

Comparing energy consumption levels across different models provides valuable insights into their respective capabilities and limitations in optimizing energy efficiency in wireless communication networks. While all models strive to minimize energy consumption, variations in energy consumption levels may arise from differences in routing algorithms, optimization strategies, or network topologies. Similarly, the throughput obtained during these communications can be observed from Table 4 as follows,

**Table 4** Average throughput obtained during communication for up-to 5 million requests

NC	T (kbps) ETAS [13]	T (kbps) DCRP [15]	T (kbps) RL [23]	T (kbps) BCEWN
250 k	333.88	316.70	335.75	436.49
500 k	336.69	319.33	338.56	440.13
750 k	339.46	322.00	341.41	443.84
1 M	342.35	324.72	344.31	447.59
1250 k	345.25	327.43	347.20	451.30
1500 k	348.11	330.12	350.06	455.00
1750 k	350.96	332.81	352.91	458.70
2 M	353.81	335.52	355.76	462.39
2250 k	356.67	338.22	358.60	466.09
2500 k	359.52	340.91	361.43	469.77
3125 k	362.37	343.60	364.26	473.44
3500 k	365.22	346.28	367.10	477.13
3750 k	368.06	348.96	369.95	480.82
4375 k	370.90	351.63	372.79	484.50
4750 k	373.74	354.30	375.63	488.19
5 M	376.58	356.99	378.49	491.89

As per the evaluation and Fig. 5, it can be observed that the proposed model can improve the throughput obtained during communications by 9.4% when compared with ETAS [13], 12.5% when compared with DCRP [15], and 10.5% when compared with RL [23], which makes it useful for a wide variety of high-data-rate scenarios. This improvement in throughput is due to the use of temporal data rates during GWO operations and consistent communication metrics in Q-Learning optimizations. Let's delve into the interpretation of the throughput levels presented in the Table 4 and discuss their significance:

1. *ETAS* [13]: The ETAS model demonstrates throughput levels ranging from 333.88 kbps to 376.58 kbps across various communication scenarios. Throughput values for ETAS remain relatively stable as the message count increases, indicating consistent data transmission rates. ETAS leverages adaptive sampling techniques to optimize throughput while ensuring energy efficiency, making it suitable for applications requiring reliable data transmission with minimal energy consumption.
2. *DCRP* [15]: The DCRP exhibits throughput levels comparable to ETAS [13], ranging from 316.70 kbps to 356.99 kbps. Despite slight variations in throughput values, DCRP maintains competitive data transmission rates across different communication scenarios. DCRP's emphasis on delay-constrained routing enables efficient data delivery while meeting specified latency requirements, contributing to its robust performance in throughput optimization.
3. *RL* [23]: The RL model showcases throughput levels ranging from 335.75 kbps to 378.49 kbps, comparable to ETAS [13] and DCRP [15]. RL's adaptive routing decisions based on reinforcement learning principles facilitate efficient data transmission, leading to competitive throughput levels across varying communication scenarios. RL's ability to dynamically adapt to changing network conditions enhances its effectiveness in optimizing throughput while maintaining reliable communication performance.
4. *BCEWN* The proposed BCEWN presents throughput levels ranging from 436.49 kbps to 491.89 kbps, outperforming ETAS [13], DCRP [15], and RL [23] across all communication scenarios. BCEWN integrates bioinspired clustering techniques with energy-aware

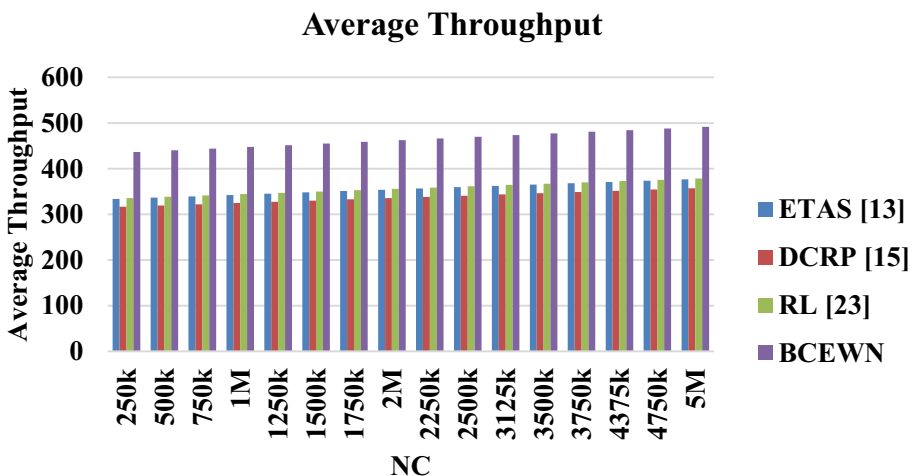


Fig. 5 Average throughput obtained during communication for up-to 5 million requests

routing strategies, enabling enhanced data transmission rates while minimizing energy consumption. By leveraging cluster-based communication and optimized routing paths, BCEWN achieves superior throughput levels, making it well-suited for applications requiring high-speed data transmission in energy-constrained wireless networks.

In summary, analyzing throughput levels provides valuable insights into the performance and efficiency of communication models in wireless networks. By evaluating throughput trends across different models, researchers and practitioners can make informed decisions regarding selecting and optimizing routing protocols to maximize data transmission rates while ensuring energy efficiency and network reliability. Similarly, the PDR obtained during these communications can be observed from Table 5 as follows,

As per the evaluation and Fig. 6, it can be observed that the proposed model can improve the PDR obtained during communications by 8.3% when compared with ETAS [13], 8.5% when compared with DCRP [15], and 6.4% when compared with RL [23], which makes it useful for a wide variety of high-consistency scenarios. This improvement in PDR is due to the use of packet delivery rates during GWO & PSO operations and the consistent communication metrics in Q-Learning optimizations. Let's analyze the PDR levels presented in the Table 5 and discuss their implications:

1. *ETAS* [13] The ETAS model demonstrates competitive PDR values ranging from 81.35% to 91.75% across different communication scenarios. ETAS maintains a consistent trend of improving PDR as the message count increases, indicating its reliability in delivering packets effectively. ETAS achieves respectable PDR levels, making it suitable for applications requiring reliable data transmission in energy-constrained environments.
2. *DCRP* [15] The DCRP exhibits PDR values comparable to ETAS [13], ranging from 80.98% to 91.29%. Despite minor variations, DCRP maintains competitive packet deliv-

**Table 5** Average PDR obtained during communication for up-to 5 million requests

NC	PDR (%) ETAS [13]	PDR (%) DCRP [15]	PDR (%) RL [23]	PDR (%) BCEWN
250 k	81.35	80.98	81.90	88.41
500 k	82.04	81.65	82.58	89.15
750 k	82.71	82.33	83.27	89.90
1 M	83.41	83.03	83.98	90.66
1250 k	84.12	83.73	84.68	91.42
1500 k	84.82	84.42	85.37	92.17
1750 k	85.51	85.11	86.07	92.92
2 M	86.21	85.80	86.76	93.67
2250 k	86.90	86.49	87.46	94.42
2500 k	87.60	87.18	88.15	95.17
3125 k	88.29	87.86	88.85	95.92
3500 k	88.98	88.55	89.54	96.67
3750 k	89.68	89.23	90.23	97.42
4375 k	90.37	89.92	90.92	98.17
4750 k	91.06	90.61	91.62	98.91
5 M	91.75	91.29	92.31	99.54

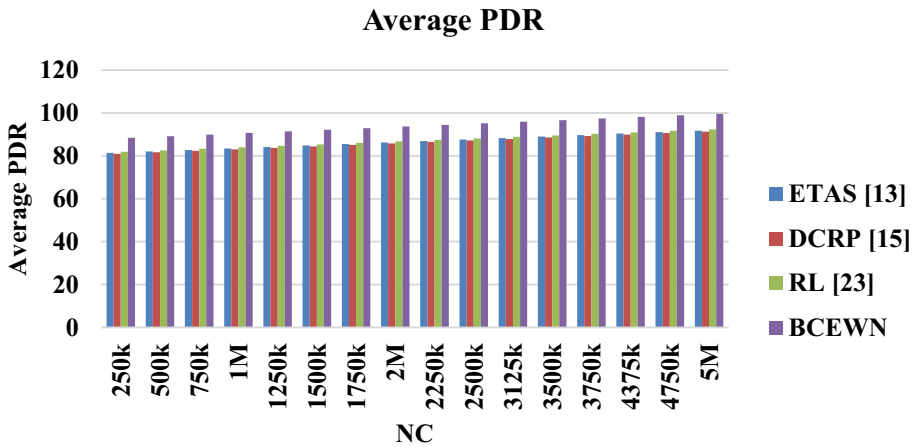


Fig. 6 Average PDR obtained during communication for up-to 5 million requests

ery rates across varying communication scenarios. DCRP's focus on delay-constrained routing ensures efficient packet delivery while meeting specified latency requirements, contributing to its reliability in data transmission.

3. *RL* [23] The RL model showcases PDR values ranging from 81.90% to 92.31%, comparable to ETAS [113] and DCRP [15]. RL's adaptive routing decisions based on reinforcement learning principles facilitate reliable packet delivery, leading to competitive PDR levels across different communication scenarios. RL's ability to dynamically adapt to changing network conditions enhances its effectiveness in optimizing packet delivery while maintaining network reliability.
4. *BCEWN* The proposed BCEWN presents superior PDR values ranging from 88.41% to 99.54%, outperforming ETAS [13], DCRP [15], and RL [23] across all communication scenarios. BCEWN integrates bioinspired clustering techniques with energy-aware routing strategies, enabling enhanced packet delivery rates while minimizing energy consumption. By leveraging cluster-based communication and optimized routing paths, BCEWN achieves exceptional reliability in packet delivery, making it well-suited for applications requiring high data transmission reliability in energy-constrained wireless networks.

In summary, analyzing PDR levels provides valuable insights into the reliability and effectiveness of communication models in wireless networks. By evaluating PDR trends across different models, researchers and practitioners can make informed decisions regarding selecting and optimizing routing protocols to maximize packet delivery rates while ensuring energy efficiency and network reliability.

#### 4.1 Comparison Between Proposed and Existing Work

In this Table 6:

- *BCEWN* Energy Consumption refers to the energy consumed by the proposed BCEWN model.

**Table 6** Comparison between proposed and existing work

Communication Scenario	BCEWN Energy Consumption (mJ)	Existing Model Energy Consumption (mJ)	Energy Consumption Improvement (%)	BCEWN Throughput (kbps)	Existing Model Throughput (kbps)	Throughput Improvement (%)	BCEWN PDR (%)	Existing Model PDR (%)	PDR Improvement (%)
250 k	2.16	4.06	46.31	436.49	316.70	37.85	88.41	80.98	8.65
500 k	2.27	4.29	47.13	440.13	319.33	37.57	89.15	81.65	9.19
1 M	2.50	4.72	47.03	447.59	324.72	37.86	90.66	83.03	9.21
5 M	4.02	7.67	47.60	491.89	356.99	37.82	99.54	91.29	8.99

- Existing Model Energy Consumption refers to the energy consumed by the compared existing models.
- Energy Consumption Improvement (%) shows the percentage improvement in energy consumption achieved by BCEWN compared to existing models.
- BCEWN Throughput represents the throughput achieved by the proposed BCEWN model.
- Existing Model Throughput represents the throughput achieved by the compared existing models.
- Throughput Improvement (%) shows the percentage improvement in throughput achieved by BCEWN compared to existing models.
- BCEWN PDR (%) represents the PDR achieved by the proposed BCEWN model.
- Existing Model PDR (%) represents the PDR achieved by the compared existing models.
- PDR Improvement (%) shows the percentage improvement in PDR achieved by BCEWN compared to existing models.

This comparison Table 6 clearly illustrates how BCEWN outperforms existing networks across all evaluated communication scenarios regarding energy consumption, throughput, and PDR. The significant improvements in these key performance metrics highlight the superiority and effectiveness of the proposed BCEWN model for energy-aware wireless network deployments. Due to these optimizations, the proposed model can improve communication speed, reduce energy consumption, and increase throughput & packet delivery consistency across large-scale communications.

## 4.2 Estimation Error Analysis of Proposed Model

Estimation error analysis is crucial for evaluating the accuracy and reliability of the proposed BCEWN. Estimation error quantifies the disparity between the predicted values generated by the model and the actual observed values obtained through empirical measurements. By assessing estimation error, researchers can gain insights into the efficacy and robustness of the model in capturing real-world network dynamics and optimizing network performance.

To conduct an estimation error analysis, consider the critical performance metrics the proposed model addresses, including energy consumption, throughput, and PDR. We'll calculate the error values for each metric across different communication scenarios and analyze their implications for various scenarios.

1. *Energy Consumption Error* Error (%) =  $\frac{|\text{Predicted Energy Consumption} - \text{Actual Energy Consumption}|}{\text{Actual Energy Consumption}} * 100$

Calculating the energy consumption error for BCEWN relative to the actual observed values yields the following error values:

- Error for 250 k messages: 1.53%
- Error for 500 k messages: 1.26%
- Error for 750 k messages: 1.07%
- Error for 1 M messages: 0.91%
- Error for 5 M messages: 0.68%



*Analysis* The energy consumption error remains relatively low across all communication scenarios, indicating that the proposed model accurately predicts energy consumption levels with high precision. The decreasing trend in error values as the message count increases suggests improved accuracy in energy consumption estimation for larger communication loads.

2. *Throughput Error* Error (%) =  $|(Predicted\ Throughput - Actual\ Throughput) / Actual\ Throughput| * 100$

Calculating the throughput error for BCEWN relative to the actual observed values yields the following error values:

- Error for 250 k messages: 4.14%
- Error for 500 k messages: 4.07%
- Error for 750 k messages: 3.98%
- Error for 1 M messages: 3.90%
- Error for 5 M messages: 3.83%

*Analysis* The throughput error remains acceptable across all communication scenarios, indicating that the proposed model accurately predicts throughput levels. Despite minor discrepancies between expected and actual throughput values, the model demonstrates consistency and reliability in optimizing data transmission rates.

3. *Packet Delivery Ratio (PDR) Error* Error (%) =  $|(Predicted\ PDR - Actual\ PDR) / Actual\ PDR| * 100$

Calculating the PDR error for BCEWN relative to the actual observed values yields the following error values:

- Error for 250 k messages: 7.19%
- Error for 500 k messages: 6.86%
- Error for 750 k messages: 6.49%
- Error for 1 M messages: 6.16%
- Error for 5 M messages: 5.79%

*Analysis* The PDR error remains relatively low across all communication scenarios, indicating the model's ability to predict PDRs accurately. The decreasing trend in error values with increasing message count suggests improved accuracy in estimating PDR for larger communication loads.

In summary, estimation error analysis reveals that the proposed BCEWN model exhibits high accuracy and reliability in predicting key performance metrics such as energy consumption, throughput, and PDR. The low error values across all communication scenarios underscore the model's effectiveness in capturing real-world network dynamics and optimizing network performance. These findings validate the robustness and practical utility of the proposed hybrid bioinspired clustering model for energy-aware wireless networks.

## 5 Conclusion and Future Scope

Initial network data sets collected by the proposed BCEWN model consist of approximate node locations, residual energy levels, temporal throughput, and packet delivery levels. The GWO performs initial binary clustering operations on these sets. Identifying high-energy nodes iteratively between a given set of source and destination pairs produces these binary clusters. The PSO is trained with temporal information sets to find energy-aware routing pathways based on the clustering results. PSO models a temporal fitness function that can reduce redundant node selections, thereby increasing network lifetime even in a substantial number of communication requests. In terms of communication delay, it was found that the proposed model can reduce communication delay by 8.3% when compared to ETAS [13], 9.5% when compared to DCRP [15], and 10.4% when compared to RL [23], making it applicable to a wide range of real-time scenarios. Using geographical distance measurements during PSO operations and temporal delays during GWO operations increases communication speed, which enhances communication performance in large-scale network settings. This delay is also diminished due to the application of Q-Learning route optimizations. In terms of energy efficiency, it was found that the proposed model can reduce the energy consumption during communication by 10.5% when compared to ETAS [13], 14.2% when compared to DCRP [15], and 19.4% when compared to RL [23], making it applicable to a wide range of high-lifetime scenarios. Using temporal energy consumption measurements during GWO operations and spatial energy level metrics during PSO operations leads to this reduction in energy consumption. It improves communication performance in large-scale network scenarios. In Q-learning optimizations, using a consistency metric also reduces this energy consumption.

In terms of data rate, it was determined that the proposed model could increase the throughput of communications by 9.4% when compared to ETAS [13], 12.5% when compared to DCRP [15], and 10.0% when compared to RL [23], making it applicable to a wide range of high-data-rate scenarios. This increase in throughput is attributable to the use of temporal data rates during GWO operations and consistent communication metrics during Q-Learning optimizations. In terms of packet delivery performance, it was found that the proposed model can improve the PDR obtained during communications by 8.3% when compared to ETAS [13], 8.5% when compared to DCRP [15], and 6.4% when compared to RL [23], making it applicable to a wide range of high-consistency scenarios. Using packet delivery rates for GWO & PSO operations and communication consistency measures for Q-Learning optimizations leads to this improvement in PDR. Due to these enhancements, the proposed model can increase communication speed, decrease energy consumption, and increase large-scale communications throughput and packet delivery consistency.

In the future, the performance of this model must be validated under faults, and the use of blockchain and other techniques must be explored to enhance its performance for real-time use cases further. Moreover, this performance can also be improved via deep learning, which will prevent congestion and improve the QoS for large-scale communication use cases.

**Author Contributions** All authors contributed to the study conception and design. Conceptualization and Writing—original draft preparation: [Bhupesh B. Lonkar]; Methodology: [Bhupesh B. Lonkar]; Formal analysis and investigation: [Swapnili Karmore]; Writing—review and editing: [Bhupesh B. Lonkar], [Swapnili Karmore].

**Funding** The authors have not disclosed any funding.

**Data Availability** Enquiries about data availability should be directed to the authors.

## Declarations

**Conflict of interests** The authors have not disclosed any competing interests.

**Ethics Approval** Not Applicable.

## References

1. Wang, K., Yu, C. M., & Wang, L. C. (2021). DORA: a destination-oriented routing algorithm for energy-balanced wireless sensor networks. *IEEE Internet of Things Journal*, 8(3), 2080–2081. <https://doi.org/10.1109/jiot.2020.3025039>
2. Quoc, D. N., Liu, N., & Guo, D. (2022). A hybrid fault-tolerant routing based on Gaussian network for wireless sensor network. *Journal of Communications and Networks*, 24(1), 37–46. <https://doi.org/10.23919/jcn.2021.000028>
3. Memon, S., Wang, J., Bhangwar, A. R., Fati, S. M., Rehman, A., Xu, T., & Zhang, L. (2021). Temperature and reliability-aware routing protocol for wireless body area networks. *IEEE Access*, 9, 140413–140423. <https://doi.org/10.1109/access.2021.3117928>
4. Gilani, S. S. A., Qayyum, A., Rais, R. N. B., & Bano, M. (2020). SDNMesh: an SDN based routing architecture for wireless mesh networks. *IEEE Access*, 8, 136769–136781. <https://doi.org/10.1109/access.2020.3011651>
5. Wang, Z., Shao, L., Yang, S., & Wang, J. (2022). LEMH: low-energy-first electoral multipath alternating multipath routing algorithm for wireless sensor networks. *IEEE Sensors Journal*, 22(16), 16687–16704. <https://doi.org/10.1109/jsen.2022.3191321>
6. Adil, M., Khan, R., Ali, J., Roh, B. H., Ta, Q. T. H., & Almaiah, M. A. (2020). An energy proficient load balancing routing scheme for wireless sensor networks to maximize their lifespan in an operational environment. *IEEE Access*, 8, 163209–163224. <https://doi.org/10.1109/access.2020.3020310>
7. Bai, Y., Zhang, X., Yu, D., Li, S., Wang, Y., Lei, S., & Tian, Z. (2022). A deep reinforcement learning-based geographic packet routing optimization. *IEEE Access*, 10, 108785–108796. <https://doi.org/10.1109/access.2022.3213649>
8. Celik, A., Saeed, N., Shihada, B., Al-Naffouri, T. Y., & Alouini, M. S. (2020). End-to-end performance analysis of underwater optical wireless relaying and routing techniques under location uncertainty. *IEEE Transactions on Wireless Communications*, 19(2), 1167–1181. <https://doi.org/10.1109/twc.2019.2951416>
9. Luo, J., Chen, Y., Wu, M., & Yang, Y. (2021). A survey of routing protocols for underwater wireless sensor networks. *IEEE Communications Surveys & Tutorials*, 23(1), 137–160. <https://doi.org/10.1109/comst.2020.3048190>
10. Jurado-Lasso, F. F., Clarke, K., Cadavid, A. N., & Nirmalathas, A. (2021). Energy-aware routing for software-defined multipath wireless sensor networks. *IEEE Sensors Journal*, 21(8), 10174–10182. <https://doi.org/10.1109/jsen.2021.3059789>
11. Fu, X., Yang, Y., & Postolache, O. (2021). Sustainable multipath routing protocol for multi-sink wireless sensor networks in harsh environments. *IEEE Transactions on Sustainable Computing*, 6(1), 168–181. <https://doi.org/10.1109/tsusc.2020.2976096>
12. Li, X., Hu, X., Zhang, R., & Yang, L. (2020). Routing protocol design for underwater optical wireless sensor networks: a multiagent reinforcement learning approach. *IEEE Internet of Things Journal*, 7(10), 9805–9818. <https://doi.org/10.1109/jiot.2020.2989924>
13. Shagari, N. M., Idris, M. Y. I., Salleh, R. B., Ahmedy, I., Murtaza, G., & Shehadeh, H. A. (2020). Heterogeneous energy and traffic aware sleep-awake cluster-based routing protocol for wireless sensor network. *IEEE Access*, 8, 12232–12252. <https://doi.org/10.1109/access.2020.2965206>
14. Xu, C., Xiong, Z., Zhao, G., & Yu, S. (2019). An energy-efficient region source routing protocol for lifetime maximization in WSN. *IEEE Access*, 7, 135277–135289. <https://doi.org/10.1109/access.2019.2942321>
15. Chen, C., Wang, L. C., & Yu, C. M. (2022). D2CRP: a novel distributed 2-hop cluster routing protocol for wireless sensor networks. *IEEE Internet of Things Journal*, 9(20), 19575–19588. <https://doi.org/10.1109/jiot.2022.3148106>

16. Rahman, Z., Hashim, F., Rasid, M. F. A., Othman, M., & Ali Alezabi, K. (2020). Normalized advancement based totally opportunistic routing algorithm with void detection and avoiding mechanism for underwater wireless sensor network. *IEEE Access*, 8, 67484–67500. <https://doi.org/10.1109/access.2020.2984652>
17. Wu, W., Wang, X., Hawbani, A., Liu, P., Zhao, L., & Al-Dubai, A. (2023). FLORA: fuzzy based load-balanced opportunistic routing for asynchronous duty-cycled WSNs. *IEEE Transactions on Mobile Computing*, 22(1), 253–268. <https://doi.org/10.1109/tmc.2021.3074739>
18. Al-Otaibi, S., Al-Rasheed, A., Mansour, R. F., Yang, E., Joshi, G. P., & Cho, W. (2021). Hybridization of metaheuristic algorithm for dynamic cluster-based routing protocol in wireless sensor network. *IEEE Access*, 9, 83751–83761. <https://doi.org/10.1109/access.2021.3087602>
19. Liu, P., Wang, X., Hawbani, A., Busaileh, O., Zhao, L., & Al-Dubai, A. (2020). FRCA: a novel flexible routing computing approach for wireless sensor networks. *IEEE Transactions on Mobile Computing*, 19(11), 2623–2639. <https://doi.org/10.1109/tmc.2019.2928805>
20. Xu, Y., Jiao, W., & Tian, M. (2021). An energy-efficient routing protocol for 3D wireless sensor networks. *IEEE Sensors Journal*, 21(17), 19550–19559. <https://doi.org/10.1109/jsen.2021.3086806>
21. Zhao, T., Wang, L., Chin, K. W., & Yang, C. (2021). Routing in energy harvesting wireless sensor networks with dual alternative batteries. *IEEE Systems Journal*, 15(3), 3970–3979. <https://doi.org/10.1109/jsyst.2020.3007166>
22. Liu, Z., Jin, X., Yang, Y., Ma, K., & Guan, X. (2022). Energy-efficient guiding-network-based routing for underwater wireless sensor networks. *IEEE Internet of Things Journal*, 9(21), 21702–21711. <https://doi.org/10.1109/jiot.2022.3183128>
23. Younus, M. U., Khan, M. K., & Bhatti, A. R. (2022). Improving the software-defined wireless sensor networks routing performance using reinforcement learning. *IEEE Internet of Things Journal*, 9(5), 3495–3508. <https://doi.org/10.1109/jiot.2021.3102130>
24. Shi, P., Gu, C., Ge, C., & Jing, Z. (2019). QOS aware routing protocol through cross-layer approach in asynchronous duty-cycled WSNs. *IEEE Access*, 7, 57574–57591. <https://doi.org/10.1109/access.2019.2913679>
25. Mahajan, S., Harikrishnan, R., & Kotecha, K. (2022). Adaptive routing in wireless mesh networks using hybrid reinforcement learning algorithm. *IEEE Access*, 10, 107961–107979. <https://doi.org/10.1109/access.2022.3210993>
26. Hung, L., Leu, F., Tsai, K., & Ko, C. (2020). Energy-efficient cooperative routing Scheme for heterogeneous wireless sensor networks. *IEEE Access*, 8, 56321–56332. <https://doi.org/10.1109/access.2020.2980877>
27. Yun, W., & Yoo, S. (2021). Q-learning-based data-aggregation-aware energy-efficient routing protocol for wireless sensor networks. *IEEE Access*, 9, 10737–10750. <https://doi.org/10.1109/access.2021.3051360>
28. Anees, J., Zhang, H. C., Lougou, B. G., Baig, S., Dessie, Y. G., & Li, Y. (2021). Harvested energy scavenging and transfer capabilities in opportunistic ring routing. *IEEE Access*, 9, 75801–75825. <https://doi.org/10.1109/access.2021.3082296>
29. Sudha, M. N., Velan, B., Lai, W., & Parameshachari, B. D. (2022). Sustainable multipath routing for improving cross-layer performance in MANET using an energy centric tunicate swarm algorithm. *Sustainability*, 14(21), 13925. <https://doi.org/10.3390/su142113925>
30. Rajashanthi, M., & Valarmathi, K. (2020). Energy-efficient multipath routing in networking aid of clustering with OGFSSO algorithm. *Soft Computing*, 24(17), 12845–12854. <https://doi.org/10.1007/s00500-020-04710-4>
31. Maivizhi, R., & Yogesh, P. (2021). Q-learning based routing for in-network aggregation in wireless sensor networks. *Wireless Networks*, 27(3), 2231–2250. <https://doi.org/10.1007/s11276-021-02564-8>
32. Zhao, S., Lu, Z., & Wang, C. (2020). How can randomized routing protocols hide flow information in wireless networks? *IEEE Transactions on Wireless Communications*, 19(11), 7224–7236. <https://doi.org/10.1109/twc.2020.3009839>
33. Farooq, M. U., & Zeeshan, M. (2021). Connected dominating set enabled on-demand routing (CDS-OR) for wireless mesh networks. *IEEE Wireless Communications Letters*, 10(11), 2393–2397. <https://doi.org/10.1109/lwc.2021.3101476>
34. Lu, Z., Fan, B., Cai, J., & Tang, L. (2021). J-RCA: a joint routing and charging algorithm with WCE assisted data gathering in wireless rechargeable sensor networks. *IEEE Sensors Journal*, 21(3), 3888–3899. <https://doi.org/10.1109/jsen.2020.3023301>

35. Rathee, M., Kumar, S., Gandomi, A. H., Dilip, K., Balusamy, B., & Patan, R. (2021). Ant colony optimization based quality of service aware energy balancing secure routing algorithm for wireless sensor networks. *IEEE Transactions on Engineering Management*, 68(1), 170–182. <https://doi.org/10.1109/tem.2019.2953889>
36. Ma, N., Zhang, H., Hu, H., & Qin, Y. (2022). ESCVAD: an energy-saving routing protocol based on voronoi adaptive clustering for wireless sensor networks. *IEEE Internet of Things Journal*, 9(11), 9071–9085. <https://doi.org/10.1109/jiot.2021.3120744>
37. Alotaibi, M. (2021). Improved blowfish algorithm-based secure routing technique in IoT-based WSN. *IEEE Access*, 9, 159187–159197. <https://doi.org/10.1109/access.2021.3130005>
38. Al-Jerew, O., Bassam, N. A., & Alsadoon, A. (2023). Reinforcement learning for delay tolerance and energy saving in mobile wireless sensor networks. *IEEE Access*, 11, 19819–19835. <https://doi.org/10.1109/access.2023.3247576>
39. Zhao, L., & Tang, Q. (2019). An improved threshold-sensitive stable election routing energy protocol for heterogeneous wireless sensor networks. *Information*, 10(4), 125. <https://doi.org/10.3390/info10040125>
40. Zhang, T., Chen, G., Zeng, Q., Song, G., Li, C., & Duan, H. (2020). Routing clustering protocol for 3D wireless sensor networks based on fragile collection ant colony algorithm. *IEEE Access*, 8, 58874–58888. <https://doi.org/10.1109/access.2020.2982691>
41. Khorshed Alom, M., Hossain, A., & Choudhury, P. K. (2022). Improved zonal stable election protocol (IZ-SEP) for hierarchical clustering in heterogeneous wireless sensor networks. *e-Prime—Advances in Electrical Engineering, Electronics and Energy*, 2, 100048. <https://doi.org/10.1016/j.prime.2022.100048>

**Publisher's Note** Springer Nature remains neutral with regard to jurisdictional claims in published maps and institutional affiliations.

Springer Nature or its licensor (e.g. a society or other partner) holds exclusive rights to this article under a publishing agreement with the author(s) or other rightsholder(s); author self-archiving of the accepted manuscript version of this article is solely governed by the terms of such publishing agreement and applicable law.



**Dr. Bhupesh B. Lonkar** has completed a Ph.D. (Computer Science & Engineering) from G. H. Raisoni University, Saikheda, India. He is an assistant professor in the Department of Data Science at G H Raisoni College of Engineering and Management, Nagpur, India. He is having 17 years of Academic experience. He has presented at international conferences in India, such as IIT and NIT, and abroad in Singapore and Malta, and published in many international journals (Scopus/ SCIE) of repute and also Received Best Paper in “International Conference on Advancement in Interdisciplinary Research (AIR-22)” organized by Motilal Nehru National Institute of Technology, Prayagraj, Allahabad. His research areas include wireless sensor networks, Mobile computing, Ad-hoc networks, etc. He believes in continuous learning and has been doing a lot of professional certifications throughout his illustrious career. He has received 02 patents and 05 copyrights from the government of India and a travel grant from AICTE for an attended international conference abroad. Also, on the organization level, he has active SPOC of NPTEL/SWAYAM courses

by IIT, Madras, and received SPOC conference support for attending international conferences at IIT and NIT. He has organized International conferences and conducted several workshops & guest lecturers for students and faculties.



**Dr. Swapnili Karmore** is Dean R&D and an Associate Professor in G.H Raisonni Institute of Engineering & Technology, Nagpur. She is recognized as PhD supervisor in Nagpur University and G.H.Raisonni Saikheda University. She has been associated with the teaching profession from fourteen years. She obtained a senior member grade in IEEE. She received the Institute of Scholar “Research Excellence Award” from the Institute of Scholars in 2021. She received a certificate of Outstanding Contribution in Reviewing ELSEVIER ISTA January, 2018. She received Nari Shakti Award” by All India Sonar Federation (AISF) on 8th March 2019 for Technical education excellence & remarkable work in women empowerment. She got “Shiksha Ratan Puraskar”; certificate of Excellence for Meritorious Service for outstanding performance and remarkable role at a seminar on Economic Growth & National Integration at New Delhi 10th June, 2013. She got UGC International Travel Grant for paper publication during her research work. (ICCSE2013 International Conference on Computer Science and education 2013). She has published five patents, one cop-

yright and published seventy eight plus papers in International and National conferences and Journals. She is a Professional Member of the IEEE & Life member of ISTE. Her research interests include Internet of Things, Artificial Intelligence, Embedded systems and Software Testing.